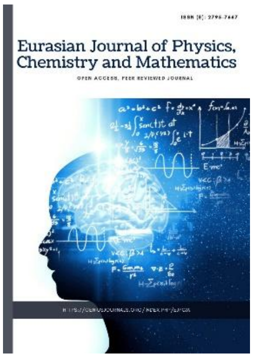

Scientific Fundamentals Of The Propane-Butane Fraction Pyrolysis Process

Sanjar H. Saidqulov
Laboratory assistant, Department of Polymer Chemistry and Chemical Technologies, Institute of Biochemistry, Samarkand State University named after Sharof Rashidov, Samarkand, Uzbekistan

Normurot I. Fayzullayev
Doctor of Chemical Sciences, Professor, Samarkand State University named after Sharof Rashidov, Institute of Biochemistry, Department of Polymer Chemistry and Chemical Technologies, Samarkand, Uzbekistan

Khamdam I. Akbarov
Doctor of Chemical Sciences, Professor, National University of Uzbekistan, Department of Physical Chemistry, Tashkent, Uzbekistan

Hayitali N. Ibodullayev
Student, Institute of Biochemistry, Samarkand State University named after Sharof Rashidov, Samarkand, Uzbekistan

ABSTRACT

This study investigates the pyrolysis of propane-butane fractions at high temperatures in an oxygen-free environment, focusing on primary reactions such as dehydrogenation, thermal cracking, radical cleavage, and aromatisation. Secondary processes, including olefin dimerisation, alkylation, and dehydroaromatization, were assessed via Gibbs free energy (ΔG°) analysis. Thermodynamic results showed that aromatisation becomes favourable around 900–1000 °C, while hydrogen release occurs above 1100 °C. Brønsted and Lewis acid sites in high-silica mesoporous zeolites significantly influence catalytic activity. Higher SiO_2/Al_2O_3 ratios reduce Brønsted site strength, lowering reaction rates and olefin selectivity. Kinetic compensation and isokinetic behaviour indicate mechanistic similarity across catalysts. The findings are relevant for improving olefin yields and energy efficiency in propane-butane pyrolysis processes.

Keywords: propane-butane fraction, pyrolysis, Gibbs free energy, Brønsted acidity, aromatisation.

Introduction

The thermal cracking process is a fundamental and large-scale operation widely applied in the petrochemical industry to convert feedstocks into valuable intermediates. The optimisation of this process typically follows two main strategies: modernisation of technological infrastructure and equipment [1–3], and enhancement of the cracking reaction itself [4–7]. These improvements often involve the use of catalytic systems [8–11] and the development of optimal reaction regimes through deterministic

[11–16] and stochastic [11, 17, 18] mathematical modelling approaches.

Deterministic modelling of thermal cracking is of particular interest due to its potential to provide a comprehensive analysis of the process and to facilitate the formulation of optimisation strategies. To generate an adequate understanding of the simulated reaction system, the application of detailed mathematical models is recommended. The scope of such models is typically defined by the theoretical representation of the chemical reaction pathways involved in hydrocarbon thermal decomposition [19–26].

However, the structure and complexity of kinetic models differ significantly among researchers studying the thermal cracking process [27–33]. Given the increasing global demand for energy and the associated environmental concerns, the sustainable and balanced development of the energy sector faces major challenges [34–40].

Experimental Section

This part of the study aims to investigate the mechanisms of primary and secondary reactions occurring during the high-temperature pyrolysis of propane-butane fractions, to evaluate the reactivity and selectivity in the presence of high-silica zeolites (HSMZs), and to determine the optimal process conditions.

Table 1. Experimental Conditions

Parameter	Value
Reaction temperature	700°C – 1100°C
Reaction medium	Inert (N_2)
Gas-volume quantity	100 ml/minute
Amount of catalyst	0.5 g (HSMZs of different modules)
Reaction time	30 minutes
Gas fraction	60% propane, 40% butane

The evaluation of reactions was performed based on the van't Hoff equation using standard Gibbs free energy (ΔG°). Within the temperature range of 900–1150°C, a transition of ΔG° values from positive to negative was observed, indicating favourable conditions for the formation of aromatic compounds and molecular hydrogen.

The amounts of reaction products — C_2H_4 (ethylene), C_3H_6 (propylene), benzene, toluene, and hydrogen — were quantitatively determined.

In terms of catalyst performance:

- The H-HSMZ-30 zeolite, with a lower silica modulus, exhibited higher activity but lower selectivity.
- In contrast, H-HSMZ-70 showed lower conversion rates yet demonstrated higher selectivity for desired products.

Table 1. Experimental results

Catalyst	Temperature (°C)	Conversion, (%)	Ethylene, (%)	Propylene, (%)	Benzene, (%)	Hydrogen, (%)
H-HSMZ - 30	800	88	29	21	14	5
H-HSMZ - 50	900	91	32	24	18	7

As the reaction temperature increases, the aromatisation and dehydrogenation reactions are thermodynamically promoted. The silicate module of the HSMZ affects the activity of the acid centres, determining the product selectivity and conversion. The optimal selectivity was observed for the H-HSMZ -50 catalyst at around 900–1000°C.

Results and Discussion

The pyrolysis (or thermolysis) of hydrocarbons refers to a complex set of chemical transformations that occur at high temperatures (typically within 700–1100 °C) in the absence of external oxidants. These processes follow a radical chain mechanism and consist of a network of sequential and parallel reactions. As a result, pyrolysis predominantly yields low-molecular-weight unsaturated hydrocarbons such as ethylene, propylene, butenes, along with methane, hydrogen, and aromatic compounds. This process represents a critical stage in the petroleum and gas chemical industries, serving as the primary route for the production of high-value olefins and other targeted products.

From a thermodynamic perspective, the thermal decomposition of hydrocarbons is a multi-step reaction involving phase, energy, and mass transfer, and exists in a transient or quasi-equilibrium state. Evaluating such processes requires calculating the change in isobaric-isothermal potential (ΔG°), which determines the thermodynamic feasibility of a reaction. This is expressed by the van't Hoff equation:

$$lnK_p = \frac{\Delta G^\circ}{RT} \qquad (1)$$

Where:

- K_p: equilibrium constant for gas-phase reactions (based on partial pressures),
- ΔG∘: standard Gibbs free energy change (kJ/mol),
- R: universal gas constant (8.314 J/mol·K),
- T: absolute temperature (K).

During the high-temperature pyrolysis of propane-butane fractions in an oxygen-free medium, not only do primary reactions such as dehydrogenation and cracking occur, but also a range of secondary transformations. These secondary processes are primarily associated with the high reactivity of the formed unsaturated hydrocarbons (e.g., ethylene and propylene), which engage in further transformations via dimerisation, trimerisation, alkylation, and dehydroaromatization, even in the absence of catalysts.

Key Reaction Mechanisms and Thermodynamic Assessment

- Olefins, particularly ethylene and propylene, are prone to dimerisation and trimerisation at high temperatures, leading to the formation of larger hydrocarbons.
- Alkylation involves reactions between saturated hydrocarbons (such as propane and butane) and olefins to form branched or higher-molecular-weight products.
- Dehydroaromatization of ethylene-series hydrocarbons occurs through multi-stage dehydrogenation, ultimately producing aromatic compounds like benzene, toluene, and xylene.
- C–C bond cleavage is a characteristic step in the radical-based cracking of C_3–C_4 hydrocarbons.
- Secondary dehydrogenation reactions (hydrogen removal) are thermodynamically possible only at elevated temperatures, but rarely occur in practice.

The thermodynamic probability of these secondary reactions is largely determined by the sign and magnitude of Gibbs free energy change (ΔG°):

- If $\Delta G^\circ<0$, the reaction is thermodynamically favourable and may proceed spontaneously.
- If $\Delta G^\circ>0$, the reaction is thermodynamically unfavourable and requires external energy input.

For instance:

- Ethane to ethylene dehydrogenation becomes thermodynamically feasible only above 1100 °C.
- Propylene dehydrogenation becomes favourable at temperatures above 1150 °C.
- Propylene C–C bond cleavage is viable above 800 °C.

Graphical Interpretation of ΔG°–T Behaviour

Figures 1–3 illustrate the variation in ΔG° values for various secondary reactions of ethylene-series hydrocarbons as a function of temperature. Based on these trends, the following conclusions can be drawn:

- Dimerisation reactions exhibit ΔG° > 0 at all temperatures, increasing with temperature, and thus are inhibited by heat.
- Aromatisation (dehydroaromatization) becomes feasible when ΔG° turns negative, approximately at 900–1000 °C.
- C–C bond cleavage reactions show decreasing ΔG° starting from 500 °C, reaching minimum values around 800 °C.

Implications for Propane-Butane Pyrolysis

In propane-butane pyrolysis, the olefins produced in primary reactions actively participate in secondary pathways. These include dehydroaromatization, dimerisation, and alkylation, which are thermodynamically feasible at high temperatures. However, both ΔG° values and residence time critically affect the efficiency of these transformations.

Secondary hydrogen evolution reactions are thermodynamically possible only at very high temperatures (1100–1150°C) and are therefore rarely encountered in practice. Thus, for accurate prediction and optimisation of process conditions, the ΔG°–T relationship remains the most reliable criterion for assessing reaction equilibrium and feasibility.

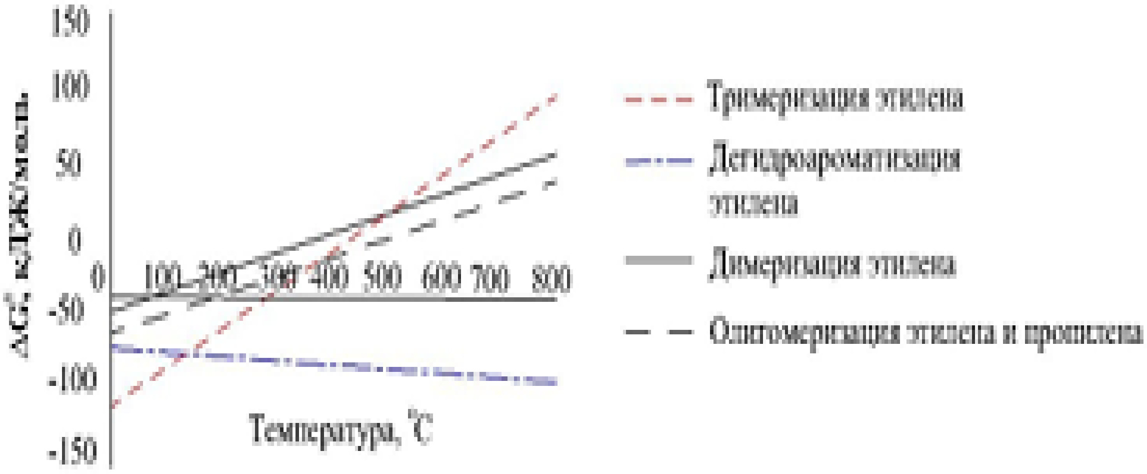

Figure 1. Effect of temperature on ΔG^0 of ethylene conversion processes.

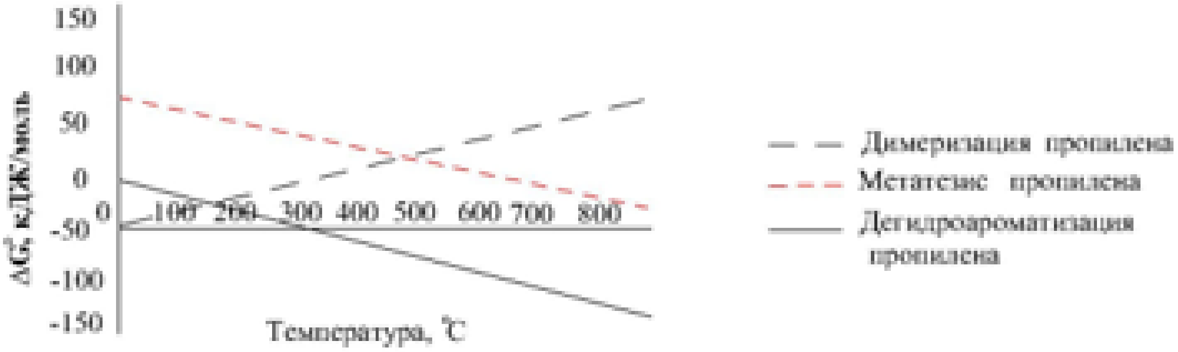

Figure 2. Effect of temperature on ΔG^0 of propylene conversion processes.

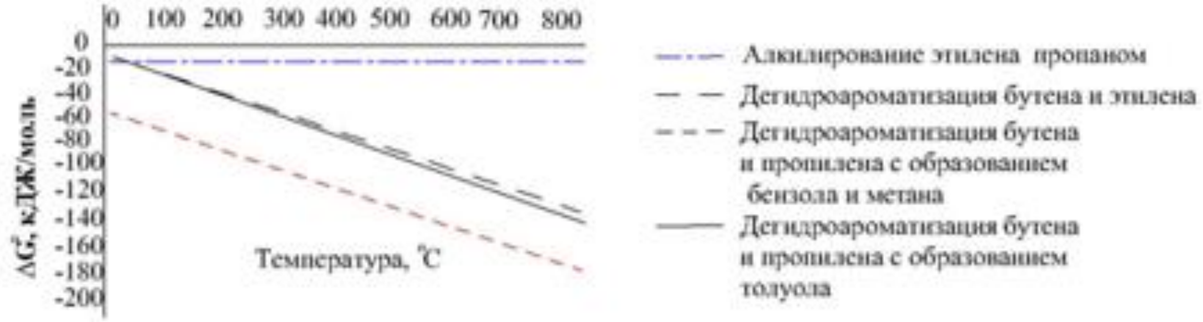

Figure 3. Effect of temperature on ΔG^0 of the conversion processes of unsaturated ethylene series hydrocarbons

The secondary reactions that occur during the decomposition of a propane-butane mixture at high temperatures in the absence of air - processes such as dehydrogenation, isomerisation, cracking, polymerisation and aromatisation - have a significant impact on the overall efficiency of the reaction. In this work, the thermodynamic potential of these reactions was analysed using the standard Gibbs free energy (ΔG°).

The following main reactions occur during the pyrolysis of propane:

1. Dehydrogenation:

$$C_3H_8 \rightarrow C_3H_6 + H_2 \quad (2)$$

2. Sequential thermal decomposition:

$$C_3H_8 \rightarrow C_2H_4 + CH_4 \quad (3)$$

3. Termination by radicals:

$$C_3H_8 \rightarrow C_2H_2 + H_2 + CH_3 \quad (4)$$

In such reactions, ethylene (C_2H_4) and propylene (C_3H_6) are the primary target products, and the reaction conditions—including temperature, pressure, and residence time—have a significant impact on their formation rates.

From a thermodynamic perspective, the pyrolysis process can be either exothermic or endothermic depending on the specific reaction pathway. For instance, the pyrolysis of ethane to produce ethylene is a strongly endothermic process that requires elevated temperatures.

$$C_2H_6 \rightarrow C_2H_4 + H_2 \Delta H^{\circ} = +137 \text{kJ/mol} \quad (5)$$

To carry out this reaction, an external heat source is required, and both the reaction rate and equilibrium conversion reach their maximum at elevated temperatures. However, increasing the temperature also enhances the likelihood of radical recombination, leading to the formation of saturated by-products or aromatic compounds.

The thermodynamics of hydrocarbon pyrolysis can be evaluated based on the stability of reaction products and their corresponding formation energies. In order to optimise the process, it is essential to calculate energy parameters, determine equilibrium constants, and conduct a thorough analysis of both the kinetic characteristics and stoichiometric relationships. Understanding these transformations plays a key role in improving the efficiency of chemical technologies and increasing the selectivity and yield of target products.

Experimental results of the conversion of propane–butane mixtures over high-silica mesoporous zeolites (HSMZs) under high-temperature and inert (oxygen-free) conditions demonstrate that the product distribution is strongly influenced by the nature of the catalytic sites, the reaction temperature, the SiO_2/Al_2O_3 ratio, and the prevailing ionic reaction mechanisms.

At temperatures below 600 °C, the low amounts of radical-derived products—such as polyaromatics, soot, and coke—suggest that the radical pathway is not dominant under these conditions. This observation supports the prevalence of an ionic (electrophilic) mechanism.

The involvement of Brønsted acid sites, specifically those associated with the Si–OH–Al groups in the H-form of aluminosilicate zeolites, plays a key role in the activation of saturated hydrocarbons (e.g., propane), facilitating the formation of carbocation intermediates.

$$C_3H_8 + H^+ \rightarrow [C_3H_9]^+ \rightarrow CH_4 + [C_3H_5]^+ \rightarrow CH_4 + C_2H_4 + H^+ \quad (6)$$

$$C_4H_{10} + H^+ \rightarrow [C_4H_{11}]^+ \rightarrow CH_4 + [C_3H_7]^+ \rightarrow CH_4 + C_3H_6 + H^+ \quad (7)$$

Lewis centre effect (de-coordinated Al centres)

$$C_3H_8 + L^+ \rightarrow LH + CH_3CH^+CH_3 \rightarrow L^+ + CH_2{=}CHCH_3 + H_2 \quad (8)$$

$$C_4H_{10} + L^+ \rightarrow LH + CH_3CH^+CH_2CH_3 \rightarrow L^+ + CH_2{=}CHCH_2CH_3 + H_2 \ (9)$$

Brønsted acid sites are responsible for C–C bond cleavage and dehydrogenation reactions (aromatisation), while Lewis acid sites facilitate hydrogen elimination and olefin formation. Secondary transformations primarily occur on Brønsted sites, although Lewis sites may also be involved. The effect of the SiO_2/Al_2O_3 ratio is significant: as this ratio increases, electron density becomes delocalized, the negative charge of $Al–O^-$ centres decreases, and the number and strength of acidic sites are reduced.

The silica modulus has a direct influence on the reaction mechanisms and the catalytic activity of HSMZs. During the conversion of propane–butane mixtures in the presence of high-silica mesoporous zeolites (HSMZs), a high silica modulus (SiO_2/Al_2O_3 ratio) not only alters the acidity profile but also affects the reaction rate and the efficiency of olefin formation.

The Brønsted acid sites in the HSMZ aluminosilicate structure (Si–OH–Al) act as proton donors, whose main function in the reaction is to activate saturated hydrocarbons and facilitate the formation of carbocation intermediates. However, as the SiO_2/Al_2O_3 ratio increases, the number of aluminium atoms decreases, electron density becomes delocalized, and the effective positive charge of the proton diminishes. As a result, the acid strength of Brønsted sites decreases. This leads to an increase in the activation energy required to generate carbocations, thereby reducing the overall reaction rate in the steps involving hydrogen removal and C–C bond cleavage, and ultimately lowering the selectivity toward olefins.

To optimise the reaction rate, selecting an appropriate SiO_2/Al_2O_3 ratio is crucial. For efficient conversion of C_3–C_4 saturated hydrocarbons into olefins, the use of HSMZs with $SiO_2/Al_2O_3 \geq 50$ is recommended. Although these catalysts possess fewer acid sites, they maintain strong and stable Brønsted centres and exhibit high thermal stability under elevated temperatures. In contrast, HSMZs with $SiO_2/Al_2O_3 \leq 30$ are less suitable for this process, as the aromatisation reactions proceed slowly, and the product composition lacks a sufficient concentration of highly unsaturated olefins.

According to long-standing experimental practice and theoretical understanding, a proportional relationship often exists between the logarithm of the pre-exponential factor (i.e., ln A in the Arrhenius equation) and the activation energy. This phenomenon is known as the kinetic compensation effect or the isokinetic relationship.

Within the scope of this study, a linear correlation was observed between $E_{ae}\phi\phi$ and ln A for reactions involving various catalyst coatings. This confirms the similarity and general nature of the underlying mechanisms, indicating that propane and butane molecules decompose via radical chain mechanisms regardless of the type of metal-based coating.

$$\boldsymbol{\beta = 1/R \cdot tg\alpha}$$

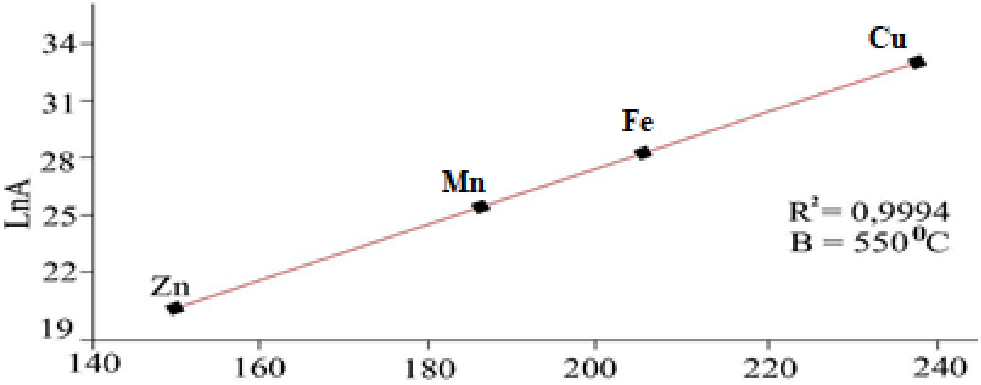

Figure 4. Dependence of the pre-exponential factor on activation energy. T – temperature, K.

Metal promoters influence the activity and selectivity of reactions inside the reactor. Zn- and Mn-modified catalysts exhibit high activity and efficiency, creating a favourable environment for the formation of C_2–C_4 unsaturated hydrocarbons. The presence of the kinetic compensation effect confirms the radical nature of the reaction mechanism and supports the promoter role of metals.

Experimentally, the isokinetic temperature for the thermal decomposition of propane–butane mixtures under oxygen-free conditions using different catalysts can be determined from the slope of the linear plot of Arrhenius parameters.

Taking into account the compensatory dependence, the equation for the propane decomposition rate constant is obtained in the following form:

$$k=\exp[-E/R(1/T-1/823)] \qquad (10)$$

Figure 4 shows that regardless of the type of catalyst used for the high-temperature decomposition of a propane-butane mixture in the absence of air, the yield of ethylene increases with increasing temperature. In the relatively low temperature range (600÷700 ℃), the type of catalyst used for the high-temperature decomposition of a propane-butane mixture in the absence of air does not have a significant effect on the yield of ethylene.

When the temperature exceeds 700℃, the catalyst used for the high-temperature decomposition of a propane-butane mixture in the absence of air becomes effective.

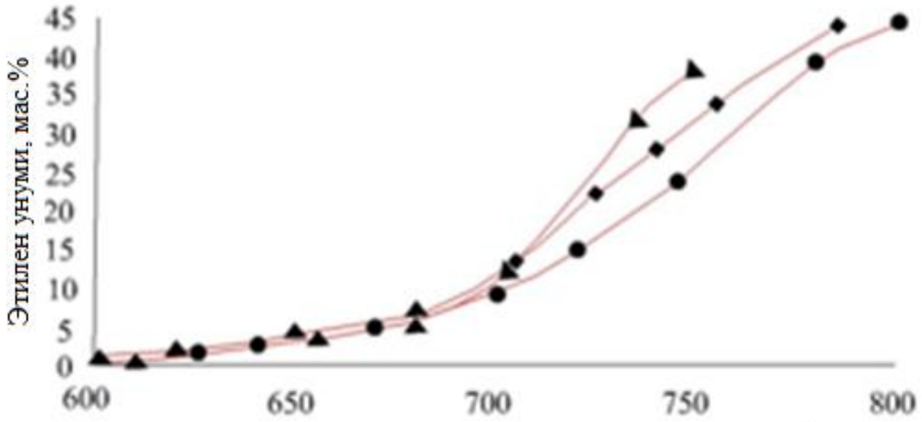

Figure 5. Ethylene productivity of selected catalysts for the decompression of various propane and butane mixture fractions at high temperature in the absence of air.

The study of the kinetic compensation effect and isokinetic relationships during the pyrolysis of propane–butane mixtures enabled a deeper understanding of the reaction mechanisms. The analysis revealed significant correlations between kinetic parameters, allowed for the calculation of activation energies, and demonstrated the importance of these factors in optimising technological processes. These findings contribute to improving the efficiency of hydrocarbon pyrolysis and serve as a foundation for the implementation of energy-saving methods.

Figure 5 illustrates the temperature dependence of the rate constant (k) for low-molecular-weight saturated hydrocarbons (propane, butane, isobutane) over H-HSMZ-50. The analysis of the results shows that propane (1) has the highest rate constant, indicating the highest reactivity; isobutane (2) demonstrates reduced reactivity due to steric hindrance; and butane (3), although structurally stable, exhibits lower reactivity compared to propane.

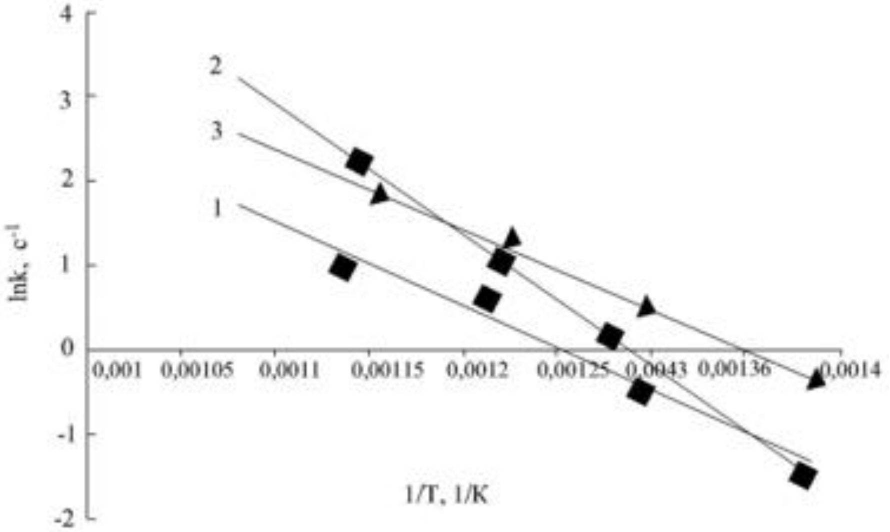

Figure 6. Effect of temperature on reaction rate constants in H-HSMZ -50.

These observations confirm that molecular structure and carbon chain branching are key factors influencing the reaction rate. In particular, the highly branched structure of isobutane limits its interaction with the active sites on the catalyst surface.

An increase in the silica modulus leads to a decrease in the proton-donating ability of Brønsted acid sites, which hinders the formation of carbocation intermediates. Consequently, the reactions involving hydrogen elimination and C–C bond cleavage slow down, reducing overall conversion efficiency. The optimal SiO_2/Al_2O_3 ratio is ≥50, which ensures both a sufficient number of acid sites and high thermal stability.

Propane exhibits higher reactivity than butane and is more readily converted into unsaturated hydrocarbons with greater rate efficiency.

The results obtained from the high-temperature conversion of propane–butane fractions over high-silica mesoporous zeolites (HSMZs) in their H-form indicate the necessity of a detailed analysis of both primary and secondary reaction mechanisms. In particular, secondary reactions have a significant impact on overall process efficiency and the selectivity toward desired products.

Selectivity and the influence of secondary transformations are especially important in reactions involving unsaturated C_2–C_4 olefins (such as ethylene, propylene, and butenes), which are considered the main target products in HSMZ-based catalytic systems. However, under high-temperature and acidic conditions, these olefins are prone to further reactions, including dehydroaromatization, isomerisation, hydrogen redistribution, polycondensation, and coking.

Conclusion

In this study, the high-temperature pyrolysis of propane–butane mixtures under inert conditions was comprehensively analysed in terms of hydrocarbon conversion processes. The mechanisms of primary and secondary reactions—including dehydrogenation, cracking, aromatisation, isomerisation, dimerisation, and alkylation—were evaluated based on their thermodynamic feasibility using standard Gibbs free energy (ΔG°) values. The analysis showed that increasing temperature enhances the thermodynamic favorability of pyrolysis reactions, with the formation of aromatic compounds becoming favourable in the 900–1000 °C range and hydrogen release becoming feasible above 1100 °C.

High-silica mesoporous zeolites (HSMZs) were used as catalysts, and it was found that their silica modulus (SiO_2/Al_2O_3 ratio) significantly influences the reaction rate, product selectivity, and the nature of acid sites. The participation of Brønsted and Lewis acid sites, the formation of carbocation intermediates, C–C bond cleavage, and olefin generation were identified as key steps in the reaction mechanism. Experimental findings confirmed that propane exhibits higher reactivity than butane, while isobutane, due to its highly branched structure, shows lower activity.

The presence of the kinetic compensation effect and isokinetic relationships indicated that the overall reaction mechanism follows a radical pathway.

These findings provide a scientific and practical basis for optimising the technological parameters of pyrolysis, enhancing the selectivity of target products such as olefins, and developing energy-efficient and effective hydrocarbon conversion processes.

References

1. Swesi, Y.; Kerleau, P.; Pitault, I.; Heurtaux, F.; Ronze, D. Purification of hydrogen from hydrocarbons by adsorption for vehicle applications. Sep. Purif. Technol. 2007, 56, 25–37.
2. Shelepova, E.V.; Vedyagin, A.A.; Mishakov, I.V.; Noskov, A.S. Simulation of hydrogen and propylene coproduction in catalytic membrane reactor. Int. J. Hydrog. Energy 2015,40, 3592–3598.
3. Newborough, M.; Cooley, G. Developments in the global hydrogen market: The spectrum of hydrogen colours. Fuel Cells Bull. 2020, 16–22.
4. Al-Fatesh, A.S.; Fakeeha, A.H.; Khan, W.U.; Ibrahim, A.A.; He, S.; Seshan, K. Production of hydrogen by catalytic methane decomposition over alumina supported mono-, bi- and tri-metallic catalysts. Int. J. Hydrog. Energy 2016,41, 22932–22940
5. Chesnokov, V.V.; Chichkan, A.S. Production of hydrogen by methane catalytic decomposition over Ni–Cu–Fe/Al_2O_3 catalyst. Int. J. Hydrog. Energy 2009,34, 2979–2985.
6. Silva, R.R.C.M.; Oliveira, H.A.; Guarino, A.C.P.F.; Toledo, B.B.; Moura, M.B.T.; Oliveira, B.T.M.; Passos, F.B. Effect of support on methane decomposition for hydrogen production over cobalt catalysts. Int. J. Hydrog. Energy 2016,41, 6763–6772.
7. Syed Muhammad, A.F.; Awad, A.; Saidur, R.; Masiran, N.; Salam, A.; Abdullah, B. Recent advances in cleaner hydrogen production via thermo-catalytic decomposition of methane: Admixture with hydrocarbon.Int. J. Hydrog. Energy2018,43, 18713-18734
8. Jian, X.; Jiang, M.; Zhou, Z.; Zeng, Q.; Lu, J.; Wang, D.; Zhu, J.; Gou, J.; Wang, Y.; Hui, D.; et al. Gas-Induced Formation of Cu Nanoparticles as Catalyst for High-Purity Straight and Helical Carbon Nanofibers. ACS Nano2012,6, 8611–8619.
9. Simon, A.; Seyring, M.; Kämnitz, S.; Richter, H.; Voigt, I.; Rettenmayr, M.; Ritter, U. Carbon nanotubes and carbon nanofibers fabricated on tubular porous Al_2O_3 substrates.Carbon 2015, 90, 25–33.
10. Bayat, N.; Rezaei, M.; Meshkani, F. Methane decomposition over Ni–Fe/Al_2O_3 catalysts for production of COx-free hydrogen and carbon nanofiber. Int. J. Hydrog. Energy2016,41, 1574–1584.
11. Fakeeha, A.H.; Ibrahim, A.A.; Khan, W.U.; Seshan, K.; Al Otaibi, R.L.; Al-Fatesh, A.S. Hydrogen production via catalytic methane decomposition over alumina-supported iron catalyst. Arab. J. Chem.2018,11, 405–414.
12. Shen, Y.; Lua, A.C. Synthesis of Ni and Ni–Cu supported on carbon nanotubes for hydrogen and carbon production by catalytic decomposition of methane. Appl. Catal. B Environ.2015, 164, 61–69.

13. Ping, D.; Wang, C.; Dong, X.; Dong, Y. Co-production of hydrogen and carbon nanotubes on nickel foam via methane catalytic decomposition. Appl. Surf. Sci. 2016, 369, 299–307.
14. Karaismail oglu, M.; Figen, H.E.; Baykara, S.Z. Hydrogen production by catalytic methane decomposition over yttria doped nickel based catalysts.Int. J. Hydrog. Energy 2019,44, 9922–9929
15. Berndt, F.M.; Perez-Lopez, O.W. Catalytic decomposition of methane over Ni/SiO_2: Influence of Cu addition. React. Kinet. Mech.Catal.2016,120, 181–193.
16. Chesnokov, V.V.; Buyanov, R.A. The formation of carbon filaments upon decomposition of hydrocarbons catalysed by iron subgroup metals and their alloys. Russ. Chem. Rev.2000,69, 623–638
17. Strel'tsov, I.A.; Vinokurova, O.B.; Tokareva, I.V.; Mishakov, I.V.; Isupov, V.P.; Shubin, Y.V.; Vedyagin, A.A. Effect of the nature of a textural promoter on the catalytic properties of a nickel-copper catalyst for hydrocarbon processing in the production of carbon nanofibers. Catal. Ind.2014, 6, 176–181.
18. Bauman, Y.I.; Lysakova, A.S.; Rudnev, A.V. Mishakov, I.V.; Shubin, Y.V.; Vedyagin, A.A.; Buyanov, R.A. Synthesis of nanostructured carbon fibers from chlorohydrocarbons over Bulk Ni-Cr Alloys. Nanotechnologies Russ.2014,9, 380–385.
19. Streltsov, I.A.; Mishakov, I.V.; Vedyagin, A.A.; Melgunov, M.S. Synthesis of Carbon Nanomaterials from Hydrocarbon Raw Material on Ni/SBA–15 Catalyst. Chem. Sustain. Dev. 2014,22, 185–192.
20. 1. M.G. Kibria, N.I. Masuk, R. Safayet, H.Q. Nguyen, and M. Mourshed, "Plastic Waste: Challenges and Opportunities to Mitigate Pollution and Effective Management", *Int J Environ Res*, 2023. *17*(1): p. 20
21. L. An, Z. Kou, R. Li, and Z. Zhao, "Research Progress in Fuel Oil Production by Catalytic Pyrolysis Technologies of Waste Plastics", *Catalysts*, 2024. *14*(3): p. 212,
22. L. Dai, N. Zhou, Y. Lv, Y. Cheng, Y. Wang, Y. Liu, K. Cobb, P. Chen, H. Lei, and R. Ruan, "Pyrolysis technology for plastic waste recycling: A state-of-the-art review", *Progress in Energy and Combustion Science*, 2022. *93*: p. 101021
23. P.G.C. Nayanathara Thathsarani Pilapitiya and A.S. Ratnayake, "The world of plastic waste: A review", *Cleaner Materials*, 2024. *11*: p. 100220,
24. T.P. Haider, C. Völker, J. Kramm, K. Landfester, and F.R. Wurm, "Plastics of the future? The impact of biodegradable polymers on the environment and on society", *Angewandte Chemie International Edition*, 2019. *58*(1): p. 50-62
25. *M. Chandran, S. Tamilkolundu, and C. Murugesan,* "Conversion of plastic waste to fuel", in *Plastic waste and recycling*. 2020, Elsevier. p. 385-399,
26. R.K. Padhan and A. Sreeram, "Enhancement of storage stability and rheological properties of polyethylene (PE) modified asphalt using cross linking and reactive polymer based additives", *Construction and Building Materials*, 2018. *188*: p. 772-780,
27. I. Tsuchimoto and Y. Kajikawa, "Recycling of Plastic Waste: A Systematic Review Using Bibliometric Analysis", *Sustainability*, 2022. *14*(24): p. 16340,
28. K. Ragaert, L. Delva, and K. Van Geem, "Mechanical and chemical recycling of solid plastic waste", *Waste management*, 2017. *69*: p. 24-58.
29. K. Radhakrishnan, P. Senthil Kumar, G. Rangasamy, L. Praveen Perumal, S. Sanaulla, S. Nilavendhan, V.Manivasagan, and K. Saranya, "A critical review on pyrolysis method as sustainable conversion of waste plastics into fuels", *Fuel*, 2023. *337*: p. 126890.
30. Shukurov J., Fayzullaev N. Direct synthesis of dimethyl ether from synthesis gas //AIP Conference Proceedings. – AIP Publishing, 2024. – T. 3045. – №. 1.
31. Shukurov J., Fayzullaev N. Kinetic laws of dimethyl ether synthesis reaction //E3S Web of Conferences. – EDP Sciences, 2023. – T. 389. – C. 01037.
32. Jasur S. et al. technology of extraction of dimethyl ether from methanol //Universum: технические науки. – 2023. – №. 6-5 (111). – C. 46-49.

33. Jasur S., Normurot F. catalyst selection and technology for obtaining dimethyl ether //Universum: химия и биология. – 2023. – №. 6-2 (108). – С. 57-61.
34. Xoshimovich S. J., Ibodullayevich F. N. mahalliy xomashyolar asosida dimetilefir olishga turli omillarning ta’siri //Issue 3 of 2023 (139/1). – 2023. – Т. 3. – №. 132. – С. 5-13.
35. Xamroyev, J. X., Shukurov, J. H., Fayzullayev, N. I., Mahmudov, O. B., & Kungratov, K. A. (2021). Analysis of texture characteristics of modified and activated navbahor bentonite. Asian Journal of Multidimensional Research, 10(9), 382-393.
36. Xamroyev J. X. et al. Optimization of the acid activation process of bentonite //ACADEMICIA: An International Multidisciplinary Research Journal. – 2021. – Т. 11. – №. 9. – С. 589-597.
37. Xolmurodovich, X. J., Hoshimovich, S. J., Fayzullayev, N. I., Bolbek o’g’li, M. O., & Asliddinovich, K. K. Physicochemical and Texture Characteristics of Natural Bentonite. JournalNX, 7(10), 45-54.
38. Shukurov J. Jasur Shukurov Khoshimovich Doct modeling the production of dimethyl ether from natural gas //Scientific and Technical Journal of Namangan Institute of Engineering and Technology. – 2023. – Т. 8. – №. 4. – С. 126-137.
39. Jasur Shukurov, Normurot Fayzullayev. Kinetic Laws of the Reaction of Dimethyl Ether Synthesis from Synthesis-Gas//International Journal of Materials and Chemistry 2023, 13(1):5-10.
40. Shukurov J. Modeling the Production of Dimethyl Ether from Natural Gas//Physical Research & Engineering Technology Problems – PRETP 2024//AIP Conference Proceedings. – AIP Publishing, 2025.